

Microbial diversity responses to lead contamination concentration in agricultural soils, Lapindo mudflow area: preliminary bioremediation study

Mohammed Bosha¹, Irfan Mustafa^{2*}, Fahrul Huyop³, and Barlah Rumhayati⁴

¹Doctoral Biology program, Faculty of Natural Science and Mathematics, University of Brawijaya, Jl. Veteran, Malang City 65145, East Java, Indonesia.

²Department of Biology, Faculty of Natural Science and Mathematics, University of Brawijaya, Jl. Veteran, Malang City 65145, East Java, Indonesia.

³Department of Biosciences, Faculty of Science, Universiti Teknologi Malaysia, 81310 UTM Johor Bahru, Malaysia.

⁴Department of Chemistry, Faculty of Natural Science and Mathematics, University of Brawijaya, Jl. Veteran, Malang City 65145, East Java, Indonesia

Abstract. Lead (Pb) contamination resulting from the Lapindo mudflow in Indonesia has generated long-lasting heavy metal stress in nearby agricultural soils, persisting for over 20 years. Microbial community responses to such environmental-geological contamination remain poorly characterized within the region. This study was designed as an exploratory investigation of the impact of Lead (Pb) contamination on bacterial diversity and community composition, in order to establish baseline ecological data for future large-scale bioremediation assessments. Soil samples were collected from three locations with differing Pb contamination levels: Location 1: Glagah Arum, Location 2: Polo Gunting, and Location 3: Pond epicenter-P025A. Physicochemical parameters were analyzed, and bacterial communities were characterized using Oxford Nanopore full-length 16S rRNA gene sequencing. Alpha-diversity metrics (Shannon, Simpson, and Chao1 indices) were computed from normalized operational taxonomic unit (OTU) data to assess microbial richness and evenness. Preliminary observations suggest that the physicochemical parameters are as follows: Location 1 (low, 2.85 mg/kg), Location 2 (moderate, 3.08 mg/kg), and Location 3 (high, 11.38 mg/kg). Diversity decreased by about 30–40% with increasing Pb concentration. Community composition appeared to shift progressively from *Pseudomonadota* dominance in low Pb soils to *Bacillota* and *Thermodesulfobacteriota* in moderately contaminated sites, and to *Cyanobacteriota* (*Oscillatoriales*) in highly contaminated soils. A resilient core microbiome of 425 taxa was detected across all sites. Redundancy analysis indicated Pb concentration as the dominant environmental filter, with soil organic matter and moisture providing secondary influences. This study provides an exploratory assessment of community composition under

* Corresponding author: irfan@ub.ac.id

Pb contamination, excluding functional genes and an actual bioremediation assay, which may inform future bioremediation and ecological restoration.

1 Introduction

The 2006 Lapindo mud volcano eruption in Sidoarjo, East Java, Indonesia, released enormous volumes of metal-laden mud that buried and contaminated thousands of hectares of agricultural land. More than 180 million cubic meters of sediment containing elevated concentrations of heavy metals, including lead (Pb), have been discharged continuously into nearby farmlands [1]. Unlike industrial pollution, which is often localized and anthropogenic in origin, the Lapindo mudflow represents a geological contamination event characterized by a complex geochemical matrix and chronic exposure conditions. These prolonged inputs have significantly reshaped the region's soil fertility, crop productivity, and microbial community stability, making the Lapindo area a unique natural laboratory for studying the long-term effects of contamination [2].

Heavy metal contamination is a critical environmental problem in agricultural ecosystems because soil microorganisms are highly sensitive to metal-induced stress, yet essential for nutrient cycling, soil fertility, and ecological resilience. Among toxic metals, lead (Pb) is particularly relevant because it is non-biodegradable, highly persistent, and biologically inactive, exerting toxicity even at low concentrations. In contrast to other metals such as cadmium (Cd), mercury (Hg), or chromium (Cr), Pb tends to accumulate in the topsoil and strongly binds to soil particles, where it directly interferes with microbial enzymatic functions, membrane integrity, and gene expression [3]. These characteristics make Pb a critical model contaminant for examining microbial community responses and ecological thresholds in contaminated soils.

Previous studies have shown that heavy metal exposure reduces microbial diversity and alters community composition by favoring resistant taxa while eliminating sensitive groups. However, most research has focused on industrial or mining sites, whereas microbial ecological dynamics under chronic geological contamination remain poorly understood. The Lapindo mudflow thus provides an opportunity to investigate microbial assembly mechanisms under prolonged, natural contamination in a tropical agricultural context. The advent of next-generation sequencing technologies has enabled in-depth profiling of microbial communities that were previously inaccessible using culture-based methods, which capture only 1–5% of soil bacteria. Full-length 16S rRNA sequencing using Oxford Nanopore Technology offers high taxonomic resolution, allowing species-level identification of microbial lineages potentially adapted to Pb stress [4]. This approach is essential for identifying taxa that may serve as bioindicators of contamination intensity or as future candidates for bioremediation.

This preliminary study aimed to assess how Pb contamination influences soil bacterial diversity and community composition in agricultural lands surrounding the Lapindo mudflow. Specifically, it sought to: (1) evaluate the relationship between Pb concentration and microbial diversity along a contamination gradient; (2) identify bacterial taxa that dominate at different contamination levels; and (3) determine key soil physicochemical factors that shape microbial community structure. The results provide

This study provides an exploratory assessment of community composition under Pb contamination, excluding functional genes and an actual bioremediation assay, which may inform future bioremediation and microbial indicators relevant to soil recovery and restoration in contaminated agricultural ecosystems.

2 Material and Method

2.1 Description of Study Area

This pilot investigation was conducted between August 2023 and July 2024 in Sidoarjo Regency, East Java, Indonesia, an area directly impacted by the 2006 Lapindo mudflow disaster. The three locations, Location 1: Glagah Arum, Location 2: Polo Gunting, and Location 3: Pond epicenter-P025A, were selected based on their distance from the mudflow source to represent different Pb contamination levels (Low, moderate, and high). These locations share similar regional climatic conditions. The study area is shown in Figure 1.

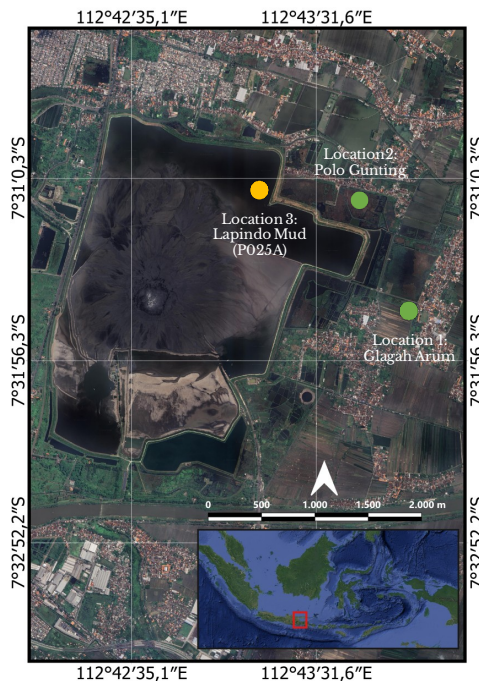


Fig. 1. Satellite image of the research location areas.

Location 1: Productive Agricultural Land (Glagaharum)

The first sampling site was situated in Glagaharum Village, within the Tangelangin District, Sidoarjo Regency, approximately 500 meters from Locations 2 and 3. This land is agriculturally productive, primarily used for rice cultivation. It relies on irrigation from the Porong River, which is known to contain elevated concentrations of heavy metals. Glagaharum Village encompasses 177 hectares, with 138 hectares dedicated to agricultural activity. The inclusion of this site allows for a comparative analysis of agricultural resilience and contaminant uptake across adjacent areas that experience

similar environmental pressures but originate from a different village. The geographical coordinates for this site are -7.3130559° latitude, 112.433192° longitude.

Location 2: Productive Agricultural Land (Pologunting)

The second sampling site was located approximately 500 meters from Location 1, within the Pologunting area of Gempolsari Village, Tanggulangin District. Similar to Location 1, this agricultural land remains productive. It is also continuously irrigated with water sourced from the Porong River, indicating sustained exposure to heavy metals. This site provides an opportunity to investigate the combined effects of the legacy mudflow impact and ongoing heavy-metal contaminated irrigation on soil characteristics and crop health. An estimated representative coordinate for this site, reflecting its adjacency to Location 1 while maintaining a distinct position, is -7.319800° latitude, 112.433000° longitude.

Location 3: Non-productive Mud Pond Area

The third sampling site was established within the Mud Pond epicenter, at Post (025A) in Gempolsari Village, Tanggulangin District, Sidoarjo Regency. This area comprises former agricultural land rendered non-productive due to significant physical damage directly attributed to its proximity to the Lapindo mudflow. Historically, this site was part of a larger 163-hectare agricultural expanse, with 65 hectares actively cultivated before the mud flooding disaster. The site's non-productive status serves as a crucial baseline for evaluating long-term environmental degradation. The geographical coordinates for this site are -7.310342° latitude, 112.42255° longitude. The strategic selection of these three sites shows variations in current productivity status and shared exposure to heavy metal-laden irrigation water from the Porong River.

2.2 Preliminary Study Design and Concept

This pilot study aimed to identify preliminary microbial diversity in Pb-contaminated soils using full-length 16S sequencing. A small sample size ($n = 3$ per site) ensured feasibility. The design focused on detecting major factors, acknowledging limited replication typical of exploratory research. The exploratory tools employed include descriptive statistics, ordination (RDA), and diversity metrics, which were used as indicators of apparent trends and confirmatory hypothesis testing.

2.3 Sampling Design

Sampling sites were selected to represent varying levels of contamination impact, agricultural productivity, and soil health. At each location, three soil samples were collected from the 0–15 cm layer. Then, they were homogenized into composite samples to reduce microsite variability. Triplicate composites ($n=3$ per site) were retained to represent within-site variability. Samples were placed in sterile containers, transported on ice, and stored at -20°C until analysis.

2.4 Soil Physicochemical Characterization

Organic matter (%) was measured with a CNS analyzer (Vario Max CN, Elementar Analysensysteme, Germany). pH and electrical conductivity (EC, mS/cm) were measured

using a pH/EC meter (Sevenmulti S40, Mettler Toledo, Switzerland). Soil water content (cm^3/cm^3) was determined by gravimetric oven-drying at 105°C to constant weight. Soil salinity (% w/w) was calculated from the residue of a 1:5 soil–water extract after evaporation to dryness according to standard procedure. Pb concentration (mg/kg) was quantified using the ICP-MS method.

2.5 Full-length 16S rRNA Gene Sequencing

2.5.1 DNA Extraction

Solid residue was collected into two centrifuge tubes to serve as replicates. DNA extraction was performed using the QIAamp® PowerFecal® Pro Kit (QIAGEN), following the manufacturer's standard protocols.

2.5.2 16S rRNA Gene Amplification and Sequencing

For bacterial community analysis, the V9 hypervariable region of the 16S rRNA gene was amplified. The primer pair used was 341F (5'-CCTACGGGNGGCWGCAG-3') and 518R (5'-ATTACCGCGGCTGCTGG-3') with inline barcodes. PCR amplification was carried out using PCR master mix under the following thermal cycling conditions: 30 cycles of denaturation at 95°C for 15 seconds, annealing at 50°C for 20 seconds, and extension at 72°C for 10 seconds [5].

2.5.3 DNA Quantification and Library Preparation

DNA concentration was determined using both a NanoDrop spectrophotometer and a Qubit fluorometer. Library preparations were conducted using kits from Oxford Nanopore Technology (ONT) [6].

2.5.4 Nanopore Sequencing and Data Processing

Nanopore sequencing was performed using MinKNOW software version 23.04.5. Basecalling was performed using Guppy version 6.5.7 with the high-accuracy model. The quality of the generated FASTQ files was visualized using NanoPlot, and subsequent quality filtering was performed using NanoFilt [7].

2.5.5 Bioinformatic Analysis

Reads were classified using the Centrifuge classifier (Kim et al., 2016). A Bacteria and Archaea index was constructed using the NCBI 16S RefSeq database (<https://ftp.ncbi.nlm.nih.gov/refseq/TargetedLoci/>). Downstream analysis and visualizations were performed using Pavian (<https://github.com/fbreitwieser/pavian>), Krona Tools (<https://github.com/marbl/Krona>), and RStudio (<https://www.R-project.org/>) with R version 4.2.3.

2.6 Statistical Analysis

The OTU/ASV table data for Phylum taxonomy level and soil parameters at three locations were normalized and analyzed using Redundancy Analysis (RDA) to determine statistical significance. Alpha diversity metrics, including Chao1, ACE, Shannon, Simpson, Inverse Simpson, and Fisher's alpha, were used to quantify microbial richness and evenness. All statistical analyses were performed in R with significance set at $p < 0.05$.

3 Results

This study provides exploratory insights into how Pb contamination associated with the Lapindo mudflow may influence soil physicochemical properties, bacterial diversity, and community assembly. The following sections combine results findings with theoretical discussion, emphasizing preliminary patterns rather than definitive conclusions due to the small sample size (n=3 per site).

3.1 Physicochemical Characteristics of Soil Samples

3.1.1 Pb Contamination as the Dominant Environmental Filter

The physicochemical analysis of the raw soil samples confirmed distinct results across the three locations (Table 1).

Table 1. Physicochemical factors of soil samples across contamination locations

Location	Pb (mg/kg)	pH	EC (mS/cm)	Salinity (%)	Water Content (cm ³ /cm ³)	Organic Matter (%)
1	2.85 ± 0.98	7.38 ± 0.32	3.70 ± 2.45	3.00	32.58 ± 3.73	9.91 ± 0.14
2	3.08 ± 1.56	7.71 ± 0.01	0.68 ± 0.19	2.00	59.78 ± 11.88	8.45 ± 1.15
3	11.38 ± 0.01	7.51 ± 0.13	2.34 ± 0.16	2.50	46.17 ± 3.73	9.17 ± 1.13

Note: Values are presented as mean ± standard deviation (SD) from 3 replicate samples per location. Parameters include lead (Pb) concentration, pH, electrical conductivity (EC), salinity, volumetric water content, and organic matter. Salinity values were constant and are reported as single values without SD. Standard deviations were estimated based on uniform distribution within the international soil quality guidelines.

Pb concentrations increased from 2.85 ± 0.98 mg/kg (Location 1) to 3.08 ± 1.56 mg/kg (Location 2) and 11.38 ± 0.01 mg/kg (Location 3). All soils were alkaline (pH 7.38–7.71). EC ranged from 0.68 to 3.70 mS/cm, salinity remained between 2–3%, moisture content ranged from 32.58 to 59.78%, and organic matter ranged from 8.45% to 9.91%.

3.2 Alpha Diversity of Microbial Communities

Alpha diversity metrics (Observed OTUs, Chao1, ACE, Shannon, Simpson, Inverse Simpson, Fisher) consistently declined along the Pb gradient (Figure 2). Location 1 exhibited the highest richness and evenness, Location 2 showed intermediate diversity, and Location 3 displayed the lowest values across all indices.

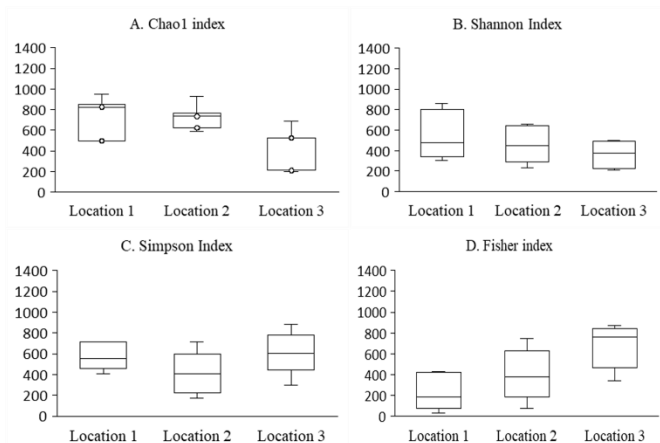


Fig. 2. The alpha diversity boxplot analysis for microbial communities across three locations. **Description:** Each index displays the variation in diversity richness (Chao, Shannon, Simpson, and Fisher) of the bacterial phylum level communities.

3.3 Taxonomic Shifts and Adaptation Mechanisms

Community composition differed markedly between sites (Table 2). Location 1 was dominated by *Pseudomonadota*. Location 2 showed increases in *Bacillota* and *Thermodesulfobacteriota*. Location 3 was dominated by *Cyanobacteria*, especially *Oscillatoriales*.

Table 2. Taxonomic dominant taxa shifts and Pb-stress mechanisms

Taxonomic Level	Location	Bacterial Taxa Present (% each)	Dominant Taxa & %
	Location 1	<i>Pseudomonadota</i> 55.45, <i>Bacteroidota</i> 8.79, <i>Actinomycota</i> 7.91, <i>Bacillota</i> 6.71, <i>Planctomycetota</i> 6.50, <i>Acidobacteriota</i> 6.29, <i>Cyanobacteriota</i> 2.36, <i>Myxococcota</i> 1.63, <i>Thermodesulfobacteriota</i> 3.59, <i>Campylobacterota</i> 0.75	<i>Pseudomonadota</i> (55.45%)
Phylum	Location 2	<i>Pseudomonadota</i> 34.82, <i>Bacillota</i> 28.25, <i>Thermodesulfobacteriota</i> 16.70, <i>Myxococcota</i> 3.60, <i>Bacteroidota</i> 3.19, <i>Planctomycetota</i> 3.15, <i>Actinomycota</i> 7.39, <i>Acidobacteriota</i> 1.94, <i>Cyanobacteriota</i> 0.74	<i>Bacillota</i> (28.25%), <i>Thermodesulfobacteriota</i> (16.70%)

	Location 3	Cyanobacteriota 66.28, Pseudomonadota 22.43, Campylobacterota 9.35, Thermodesulfobacteriota 1.31, Bacillota 0.50, Bacteroidota 0.13	Cyanobacteriota (66.28%)
	Location 1	Alphaproteobacteria 26.39, Gammaproteobacteria 24.91, Betaproteobacteria 20.84, Planctomycetia 7.61, Actinomycetes 4.69, Bacilli 4.01, Clostridia 3.84, Cyanophyceae 3.08	Alphaproteobacteria (26.39%), Gammaproteobacteria (24.91%), Betaproteobacteria (20.84%)
Class	Location 2	Bacilli 20.00, Gammaproteobacteria 19.48, Alphaproteobacteria 17.37, Clostridia 14.48, Betaproteobacteria 7.15, Desulfuromonadia 9.95, Planctomycetia 2.89, Cyanophyceae 0.94	Bacilli (20.00%), Desulfuromonadia (9.95%)
	Location 3	Cyanophyceae 67.23, Gammaproteobacteria 18.36, Epsilonproteobacteria 9.47, Alphaproteobacteria 4.25	Cyanophyceae (67.23%)
	Location 1	Burkholderiales 26.26, Xanthomonadales 20.06, Hyphomicrobiales 18.20, Bacillales 5.71, Eubacteriales 5.57, Rhodospirillales 5.93, Others 13.98, Oscillatoriales 0.97, Campylobacterales 0.90, Desulfuromonadales 1.93	Burkholderiales (26.26%), Xanthomonadales (20.06%), Hyphomicrobiales (18.20%)
Order	Location 2	Bacillales 31.54, Eubacteriales 21.99, Hyphomicrobiales 14.16, Desulfuromonadales 13.27, Rhodospirillales 6.57, Burkholderiales 4.75, Xanthomonadales 3.93, Oceanospirillales 1.61, Others 1.69	Bacillales (31.54%), Desulfuromonadales (13.27%)
	Location 3	Oscillatoriales 71.66, Oceanospirillales 14.23, Campylobacterales 9.82, Rhodospirillales 3.55, Others 0.06	Oscillatoriales (71.66%)
	Location 1	Xanthomonadaceae 61.20, Bacillaceae 8.35, Clostridiaceae 5.35, Rhodospirillaceae 4.34, Others 17.01	Xanthomonadaceae (61.20%)
Family	Location 2	Bacillaceae 44.68, Methylococcaceae 18.62, Clostridiaceae 18.14, Oceanospirillaceae 1.60, Rhodospirillaceae 3.65, Others 7.35	Bacillaceae (44.68%), Methylococcaceae (18.62%)

	Location 3	Sirenicapsillariaceae 69.45, Oceanospirillaceae 14.49, Arcobacteraceae 8.15, Rhodospirillaceae 3.51, Others 4.40	Sirenicapsillariaceae (69.45%)
--	------------	--	--------------------------------

3.4 Unique and Shared Taxa (Core Microbiome)

Venn analysis identified 2,809 unique taxa at Location 1, and 2,292 at Location 2, and 388 at Location 3. A core microbiome of 425 taxa was shared across all sites (Figure 3).

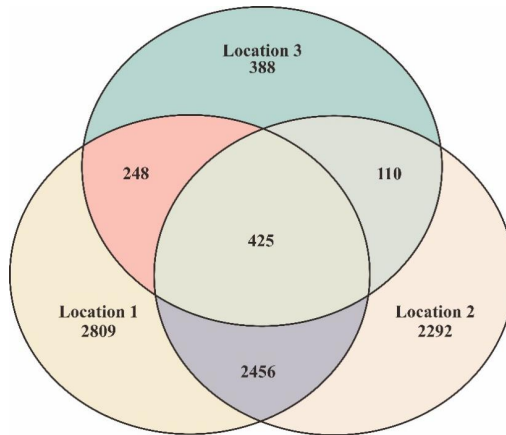


Fig. 3. Venn diagram of shared and unique microbial taxa across Locations 1, 2, and 3.

Description: The figure represents the number of taxa unique to each location or shared between two or all locations.

3.5 Environmental Drivers of Community Assembly

Redundancy Analysis (RDA) showed that Pb concentration accounted for the largest proportion of variation (~45%), followed by soil organic matter and moisture (Figure 4).

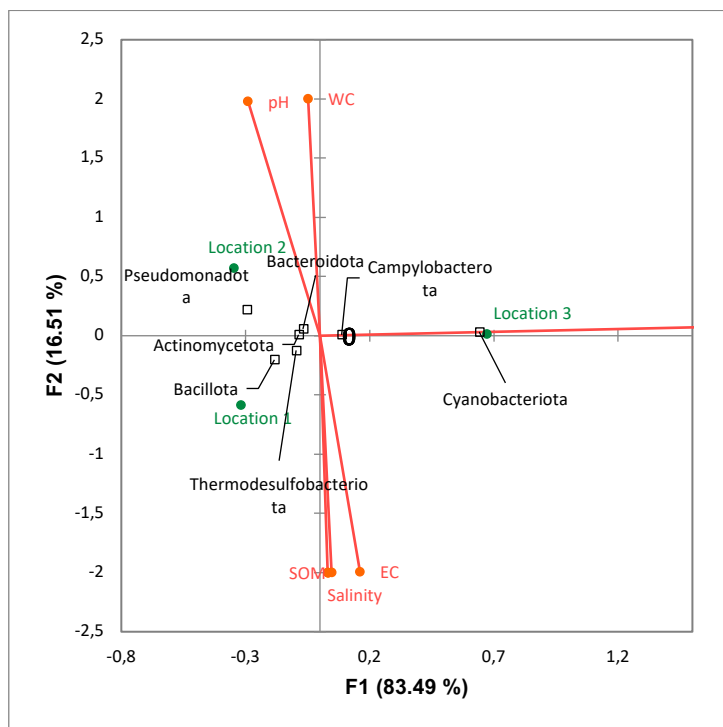


Fig. 4. The RDA (Redundancy Analysis) correlation of locations 1, 2, and 3.

4 Discussion

4.1 Pb as the Dominant Environmental Filter

The strong Pb gradient across sites indicates that contamination intensity shapes microbial assembly. Similar Pb-specific gradients in mining soils show Pb alone explaining 40–55% of community variation [8]. Highlighting Pb as a strong ecological filter. The increase from 2.85 to 11.38 mg/kg mirrors global patterns where even low-level Pb selectively removes sensitive taxa and favors resistant groups. Overall, findings show that organic matter and moisture acted as secondary modulators, likely affecting Pb concentrations by influencing metal solubility and providing metabolic substrates. Alkaline pH and high organic matter likely reduced Pb bioavailability, buffering microbial stress [9].

4.2 Decline in Diversity Under Pb Stress

The diversity indices revealed significant variations in microbial community structure across the three sites (Figure 1). This trend is consistent with other studies, where heavy metal concentrations exert a pronounced influence on bacterial diversity. Relative to the control site, the Chao1 richness estimator declined by nearly 50%, while the Shannon diversity index decreased by ~20%, indicating both a reduction in species richness and moderate losses in evenness. In addition, several bacterial genera have displayed strong correlations with specific metals; for instance, *Ramlibacter* has shown a positive association with Zn levels, whereas *Steroidobacter* has been linked with Cd

concentrations [10]. These taxa may therefore serve as potential bio-indicators for monitoring contamination and guiding soil remediation strategies. This principle is supported by evidence from industrial Pb exposure studies, where Pb exceeded 10 mg/kg within 1 km of emission hotspots showed up to 35% reductions in Shannon diversity compared to reference soils [11]. Such sharp diversity losses near contamination sources parallel the exponential decay pattern observed in Lapindo, where the closest site (0.5 km) had the highest Pb levels and the lowest diversity. The consistent decline in observed OTUs, Chao1, ACE, and diversity indices supports Hypothesis 1: increasing Pb concentration is negatively associated with bacterial diversity. The strongest losses occur among rare taxa, which provide functional redundancy and resilience.

4.3 Mechanisms Behind Taxonomic Shifts

Community composition exhibited distinct shifts along the contamination gradient (Table 2). Location 1 (low Pb) was dominated by *Pseudomonadota* (55.45%), followed by *Bacteroidota*, *Actinomycota*, and *Bacillota*. Families such as *Xanthomonadaceae* (61.2%) were enriched, consistent with traits of biofilm formation and metal adsorption [12]. Location 2 (moderate Pb) was characterized by *Bacillota* (28.25%) and *Thermodesulfobacteriota* (16.70%). Families included *Bacillaceae* (44.68%), known for spore-forming stress tolerance, and *Methylococcaceae* (18.62%), which use methane oxidation and specialized carbon metabolism. Location 3 (high Pb) was strongly dominated by *Cyanobacteriota* (66.28%), particularly *Oscillatoriales* (71.66%). The *Sirenicapsillariaceae* (69.45%) family was prevalent, with adaptations including extracellular polysaccharides and biosorption capacity [13]. These taxonomic shifts mirror findings in Pb-polluted agricultural soils in Eastern China, where *Pseudomonadota* dominated at low Pb (3–4 mg/kg), *Bacillota* increased under moderate contamination (6–8 mg/kg), and *Cyanobacteriota* prevailed in severely contaminated sites (>10 mg/kg) [11]. These results support Hypothesis 2, that severe contamination selectively favors resistant taxa, while sensitive and generalist groups decline.

4.4 Core Microbiome Stability

Comparable studies in Pb-contaminated soils across China found core microbiomes of ~400–600 taxa, including *Bacillus*, *Burkholderia*, and *Cyanobacteria* [14], suggesting convergent ecological roles, contributing to nitrogen cycling, organic degradation, and Pb immobilization [15]. These findings support Hypothesis 3: while contamination filters communities, a resilient microbial backbone persists, sustaining key ecosystem functions. In summary, Spatial comparison revealed an exponential decline in diversity near the mudflow source. This supports the proposed Contamination Distance Decay Theory, which reframes contamination intensity, not only geographic distance, as the primary driver of microbial turnover. These results revealed a clear Pb contamination gradient across the study sites, accompanied by progressive declines in microbial richness, shifts in taxonomic composition, and changes in environmental drivers of community structure. These patterns indicate strong contamination effects on bacterial diversity and assembly.

5 Conclusion

In conclusion, this investigation was an exploratory study, and accepts important limitations such as a small sample size ($n=3$ per site), single time-point sampling, and a focus on taxonomic rather than functional assessment. Microbial richness and evenness declined with increasing Pb concentrations, while resistant taxa such as *Bacillota* and *Cyanobacteriota* became dominant in heavily contaminated soils. A core microbiome persisted across all sites, suggesting a set of tolerant taxa capable of sustaining essential ecosystem functions. These constraints are appropriate for an exploratory phase, but highlight clear directions for scaling up research. Future research might involve several steps: (1) immediate follow-up studies with spatial validation, expanded to ≥ 15 replicates per contamination level across multiple transects (0.5–15 km from epicenter); (2) evaluation of temporal dynamics by implementing quarterly sampling over two years to capture seasonal variability; (3) increased analytical focus via integration of Pb speciation with community diversity analyses; (4) developing mechanistic understandings by employing multi-omics approaches -combining metagenomics, transcriptomics, and metabolomics to explore resistance mechanisms; (5) cultivation studies isolating Pb-resistant taxa (e.g., *Bacillus*, *Cyanobacteria*) and characterizing their functional potential; (6) implementation of bioremediation development - designing microbial inoculants and evaluating performance in field trials; (7) agricultural integration by assessing plant-microbe interactions under Pb stress, and testing restoration strategies for crop productivity; (8) examining how rainfall and temperature variability influence contamination impacts; (9) engaging local farmers as social-ecological integration, to assess economic viability, and incorporate traditional knowledge; and (10) extending findings to other geological contamination sites as comparative investigations for broader theoretical contributions. This staged framework would transition initial observations onto a long-term research trajectory, enabling the development of robust theories, methodological advancements, and practical solutions for Pb-contaminated agricultural ecosystems in Indonesia and beyond.

Acknowledgements

The authors would like to thank the staff of the Ecology Laboratory and the Microbiology Laboratory, Faculty of Mathematics and Natural Sciences, Universitas Brawijaya, for their technical support and field assistance. We also extend our appreciation to PT. Genetika Science Indonesia for its sequencing services. This research was conducted in accordance with institutional ethical guidelines for microbial studies. All authors have read and agree to the journal's ethical guidelines. The authors declare no conflict of interest.

Fundings

This research receives no external funding.

Data availability statement

The MinION Raw Fasta Q sequence data (filtered and merged) are available at NCBI under BioProject number PRJNA1236660.

Author contribution statement

Mohammed Bosha: Conceptualization theory; Sampling; Investigation; Writing - Original draft preparation, Data curation. Irfan Mustafa: Supervision; Sampling; Review & Editing. Fahrul Huyop:

Supervision; Writing - Review & Editing. Barlah Rumhayati: Resources; Project administration; Supervision.

References

1. S. A. Miller and A. Mazzini, *Mar. Pet. Geol.* **90**, 10 (2018).
2. U. Zulfiqar, M. Irshad, Z. Ali, M. Rizwan, S. Farid, M. Ishfaq, M. Ihsan, and M. Ahmad, *J. Environ. Manage.* **250**, 109557 (2019).
3. L. Zou, L. Chen, Y. Wu, Y. Ye, M. Zeng, Y. Du, Y. Li, and W. Wu, *Front. Environ. Sci.* **9**, 630668 (2021).
4. A. S. Parab, M. Ghose, C. S. Manohar, M. U. Gauns, and S. Paul, *Reg. Stud. Mar. Sci.* **78**, 103768 (2024).
5. K. Kumaishi, Y. Ueki, M. Kodama, S. Takahashi, T. Ito, Y. Tani, and T. Kurihara, *Sci. Rep.* **12**, 23943 (2022).
6. R. R. Wick, L. M. Judd, and K. E. Holt, *Genome Biol.* **20**, 1727 (2019).
7. B. C. Mann, J. J. Bezuidenhout, Z. H. Swanevelder, and A. F. Grobler, *Data Brief* **36**, 107036 (2021).
8. X. Hu, D. Zhang, Y. Li, H. Chen, Y. Zhang, M. Zhang, Z. Lin, and J. Wang, *Front. Microbiol.* **12**, 707786 (2021).
9. I. Sazykin, L. Khmelevtsova, T. Azhogina, and M. Sazykina, *Agriculture* **13**, 653 (2023).
10. Z. Luo, J. Ma, F. Chen, X. Li, and S. Zhang, *Int. J. Environ. Res. Public Health* **15**, 1030 (2018).
11. P. Li, L. Zhou, W. Wang, Y. Zhao, J. Zhang, L. Huang, J. Tang, and Z. Xu, *J. Hazard. Mater.* **443**, 130241 (2023).
12. M. M. Haque, M. K. Mosharaf, M. A. Haque, M. Z. H. Tanvir, and M. K. Alam, *Front. Microbiol.* **12**, 615113 (2021).
13. N. Kalita and P. P. Baruah, *J. Hazard. Mater. Adv.* **11**, 100349 (2023).
14. X. Zhong, J. Chen, Y. Ye, H. Wang, L. Li, X. Chen, L. Tang, and S. Huang, *J. Hazard. Mater.* **443**, 130241 (2023).
15. A. Patil, S. Chakraborty, Y. Yadav, B. Sharma, S. Singh, and M. Arya, *Biorem. J.* (2024). <https://doi.org/10.1080/10889868.2024.2375204>.